

# On the resonance spectra of particle-unstable light nuclei with a Sturmian approach that preserves the Pauli principle.

L. Canton<sup>(1)</sup>, K. Amos<sup>(2)</sup>, S. Karataglidis<sup>(3)</sup>, G. Pisent<sup>(1)</sup>, J. P. Svenne<sup>(4)</sup>

<sup>(1)</sup> Istituto Nazionale di Fisica Nucleare, Sez. di Padova, e  
Dipartimento di Fisica dell'Università,  
via Marzolo 8, Padova I-35131, Italia,

<sup>(2)</sup> School of Physics, The University of Melbourne,  
Victoria 3010, Australia

<sup>(3)</sup> Department of Physics and Electronics,  
Rhodes University, Grahamstown 6140, South Africa

<sup>(4)</sup> Department of Physics and Astronomy, University of Manitoba,  
and Winnipeg Institute for Theoretical Physics,  
Winnipeg, Manitoba, Canada R3T 2N2

February 9, 2008

## Abstract

The fundamental ingredients of the MCAS (multi-channel algebraic scattering) method are discussed. The main feature, namely the application of the sturmian theory for nucleon-nucleus scattering, allows solution of the scattering problem given the phenomenological ingredients necessary for the description of weakly-bound (or particle-unstable) light nuclear systems. Currently, to describe these systems, we use a macroscopic, collective model. Analyses show that the couplings to low-energy collective-core excitations are fundamental but they are physically meaningful only if the constraints introduced by the Pauli principle are taken into account. For this we introduce in the nucleon-nucleus system the Orthogonalizing Pseudo-Potential formalism, extended to collective excitations of the core. The formalism leads one to discuss a new concept, Pauli hindrance, which appears to be important especially to understand the structure of weakly-bound and unbound systems.

## 1 Sturmians

We outline here the use of Sturmian functions in the formulation of the Coupled-Channel scattering problem. Sturmians provide the solution of the scattering problems by matrix manipulation (hence the word “algebraic” in MCAS). They are known and used also in atomic and molecular physics, chemistry and field theory [1, 2]. They provide an

efficient formalism for determination of S-matrices, scattering wave functions, bound states, and resonances. They work well with non-local interactions (such as those non localities arising from the effects due to Pauli exchanges). They allow a consistent treatment of Coulomb plus nuclear interactions, as well as the inclusion in the scattering process of coupled-channel dynamics. This occurs, for instance, when strong coupling to low-lying excitations of the target nucleus have to be taken into account.

Sturmians (*also known as* Weinberg states) represent an *alternative* way to formulate the Quantum Mechanical problem.

Consider a two-body like Hamiltonian  $H = H_o + V$ : then the Schrödinger equation is written in the standard (time-independent) way

$$(E - H_o)\Psi_E = V\Psi_E, \quad (1)$$

where  $E$  is the spectral variable, and  $\Psi_E$  is the eigenstate.

Sturmians, instead, are the eigensolutions of:

$$(E - H_o)\Phi_i(E) = \frac{V}{\eta_i(E)}\Phi_i(E), \quad (2)$$

where  $E$  is a parameter. The eigenvalue  $\eta_i$  is the potential scale. Thus the spectrum consists of all the potential rescalings that give solution to that equation, for given energy  $E$ , and with well-defined boundary conditions.

The standard boundary conditions for Sturmians  $\Phi_i(E)$  are:

$E < 0$  Bound-state like; normalizable.

$E > 0$  Purely outgoing/radiating waves; non-normalizable.

The spectrum of eigenvalues is purely discrete, and bounded absolutely. For short-range (nuclear-type) potentials, the eigenvalues can accumulate around 0 only.

Then, the single-channel  $S$ -matrix can be written as

$$S(E) = \frac{\Pi_i(1 - \eta_i(E^{(-)}))}{\Pi_i(1 - \eta_i(E^{(+)})} \quad (3)$$

Alternatively, introducing the factor  $\hat{\chi}_i(E, k)$  in momentum space

$$\hat{\chi}_i(E, k) = \langle k, c | V | \Phi_i(E) \rangle, \quad (4)$$

the  $S$ -matrix can be rewritten also as

$$S(E) = 1 - i\pi k \sum_i \hat{\chi}_i(E^{(+)}; k) \frac{1}{1 - \eta_i(E^{(+)})} \hat{\chi}_i(E^{(+)}; k) \quad (5)$$

Most interestingly, the last expression can be generalized to coupled-channel dynamics: one starts from a coupled-channel Hamiltonian with potential  $V_{cc'}$ , and obtains an  $S$ -matrix of the form [3]:

$$S_{cc'}(E) = \delta_{cc'} - i\pi \sqrt{k_c k_{c'}} \sum_i \hat{\chi}_{ci}(E^{(+)}; k_c) \frac{1}{1 - \eta_i(E^{(+)})} \hat{\chi}_{c'i}(E^{(+)}; k_{c'}) \quad (6)$$

It is remarkable that the following interpretation can be given to the last expression: the scattering process initiated in the asymptotic channel  $c$  is “captured” into Sturmians. Subsequently the Sturmian propagates freely in the interaction region and finally

decays into the outgoing channels. This structure naturally reflects the description of the scattering process in terms of compound nucleus formation, and leads to an expression which is rather similar to that obtained in  $R$ -matrix formalism. However, in the Sturmian approach, such structure emerges directly from the Hamiltonian, while in the  $R$ -matrix formalism, the resonant (compound) structure is modeled phenomenologically in terms of specific boundary conditions given at the surface of an hypothetic  $R$ -space sphere.

### 1.1 Resonances and bound states in terms of Sturmians

Resonant structures as well as bound states can be obtained in terms of the properties of Sturmian eigenvalues. A bound state occurs when one of the eigenvalues moves toward the right on the real axis, and crosses the value 1 at some negative energy. That particular energy value corresponds to the bound-state energy. A resonance occurs when the eigenvalue, initially progressing along the the real axis, becomes complex before reaching the point (1,0). Such occurs for positive energies as the scattering threshold ( $E = 0$ ) must be passed. The energy centroid of the resonance is the energy corresponding to the real part of sturmian eigenvalue matching the value 1. The width of the resonance can also be determined geometrically by the patterns of the sturmian trajectories, and relates to the imaginary part of the sturmian eigenvalue at the resonant energy. Such patterns can be seen in Fig. 1. In Fig. 2 one observes the situation in a realistic case, namely  $n$ - $^{12}\text{C}$  elastic scattering. The eigenvalue trajectories produce two  $3/2^+$  resonances that can be clearly seen in the experimental data as well as in the theoretical calculation.

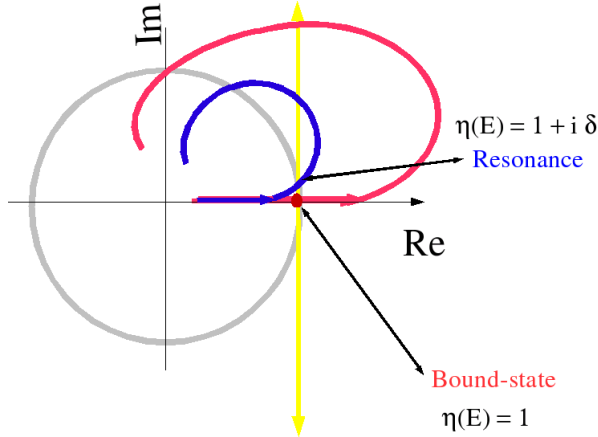


Figure 1: How resonances and bound states are found in Sturmian theory.

## 2 Model Coupled-channel potential and OPP

To date, we have used a macroscopic potential approach: a nucleon is scattered by a nucleus (light nuclei with  $0^+$  g.s. are considered) and we include couplings to first core excitations of collective nature (quadrupole, octupole, etc), since these couplings play an important role in the dynamics. The coupled-channel potential that describes the dynamics (including the couplings to collective-type target excitations) is an expansion

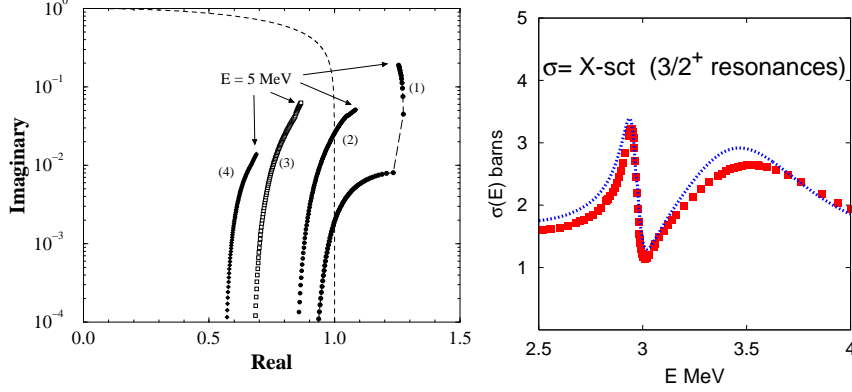


Figure 2: Neutron- $^{12}\text{C}$  in the  $3/2^+$  channel: a realistic case. Low-energy resonances in  $3/2^+$   $n$ - $^{12}\text{C}$  system. Sturmian patterns (left) and  $3/2^+$  resonant cross-section (right). The dashed line in the left panel denotes the unit circle.

over four operators, where the first two play a dominant role (central and spin-orbit), while the remaining two operators (orbit-orbit and spin-spin) produce small phenomenological corrections. The sum over the various operator forms can be written as follows [4]

$$V_{cc'}(r) = \sum_{n=C, \ell s, \ell \ell, sI} V_n \langle (\ell s) j I; J^\pi | \mathcal{O}_n f_n(r, R, \theta_{\mathbf{r}, \mathbf{R}}) | (\ell' s) j' I'; J^\pi \rangle$$

For all operators, the functional forms are expanded to second order in the core-deformation parameter. (For simplicity, we discuss here the case of a single quadrupole deformation effect:  $R = R_0(1 + \beta_2 P_2(\theta))$ .)

$$f_n(r, R, \theta) = f_n^{(0)}(r) - \beta_2 R_0 P_2(\theta) \frac{d}{dr} f_n^{(0)}(r) + \frac{\beta_2^2 R_0^2}{2\sqrt{\pi}} \left( P_0 - \frac{2\sqrt{5}}{7} P_2(\theta) + \frac{2}{7} P_4(\theta) \right) \frac{d^2}{dr^2} f_n^{(0)}(r)$$

The radial forms  $f^{(0)}(r)$  are spherically-symmetric functions.

For the central, orbit-orbit, and spin-spin terms we consider a standard Wood-Saxon form:

$$f_n^{(0)}(r) = [1 + \exp \frac{r-R}{a}]^{-1} \quad \text{for } (n = C, \ell \ell, sI) \quad (7)$$

For the spin-orbit term we consider  $\mathcal{O}_{ls} = \mathbf{l} \cdot \mathbf{s}$  and not the full Thomas term, with the following radial form:

$$f_{LS}^{(0)}(r) = \frac{1}{r} \frac{d}{dr} [1 + \exp \frac{r-R}{a}]^{-1} \quad \text{for } (ls) \quad (8)$$

## 2.1 First application: $n$ - $^{12}\text{C}$

In our first application, we considered the scattering of neutrons off  $^{12}\text{C}$  coupling the ground state of the target to the first two low-lying excitations  $2_1^+$  (4.43 MeV) and  $0_2^+$  (7.63 MeV), and searched parameters to obtain a description of the resonant spectra

and scattering cross sections [4, 5, 6]. However, many deeply-bound spurious states occurred in the bound spectrum. It was not possible to obtain a consistent description of both bound structure and scattering data with the same Coupled-Channel Hamiltonian. These spurious deeply-bound states originate from the violation of the Pauli principle. The phase-space corresponding to target nucleons in fully occupied shells has to be inhibited to the incoming nucleon. In the original CC model such condition was missing.

Various methods have been suggested to remove the deeply-bound forbidden states. A recent article [7] on the subject contains an historical review on the various approaches and their connections. In phenomenological macroscopic-type calculations, such Pauli condition has been implemented first by introducing the Orthogonality Condition Model [8]. Alternatively, the orthogonality condition can be introduced directly in the Hamiltonian by addition of a new term in the potential, the highly non-local Orthogonalizing Pseudo-Potential [9]. With the advent of super-symmetric quantum mechanics[10], it was possible to define super-symmetric transformations[11] that produce new local (and highly singular) potentials which also generate spectra free of spurious states.

In our MCAS approach, we use the technique of Orthogonalizing Pseudo Potentials [5], which eliminates the deep bound states adding a new term in the nuclear potential.

The “complete” nuclear potential for the  $n + {}^{12}\text{C}$  case we considered, has the form (in partial-wave decomposition)

$$\mathcal{V}_{cc'}(r, r') = V_{cc'}(r)\delta(r - r') + \delta_{cc'}\lambda_c A_c(r)A_c(r')(\delta_{c=s\frac{1}{2}}) + \delta_{cc'}\lambda_c A_c(r)A_c(r')(\delta_{c=p\frac{3}{2}}).$$

$A_c(r)$  are the *Pauli-forbidden* deep (CC-uncoupled) bound states. The  $\lambda$  parameter eliminates the deeply-bound spurious states, since a state in the OPP approach is forbidden in the limit  $\lambda \rightarrow +\infty$ , while it is *allowed* when  $\lambda \rightarrow 0$ .

Thus, in  ${}^{13}\text{C}$ , we considered two shells (the  $0s_{\frac{1}{2}}$  and  $0p_{\frac{3}{2}}$  shells) to be Pauli blocked.

## 2.2 The $\lambda$ -dependence

One important aspect in the OPP method is to assess the behavior with respect to the  $\lambda$  parameters. Originally,  $\lambda$  was set to 100 MeV since this was sufficient to remove all the spurious states, but later it was found that some resonances were still sensitive to higher values of  $\lambda$ , corresponding to a stronger orthogonality condition, and the energy centroids of those selected resonances improved by using larger values of  $\lambda$ . In particular, a narrow  $5/2^-$  resonance, which lies very close to threshold, illustrates this well. When  $\lambda = 100$  MeV, it is almost a zero-energy bound state. For higher values of  $\lambda$  that resonance converges to a position in agreement with the peak observed in the evaluated data around 0.1 MeV. Also the energy centroid of the  $1/2^-$  state around 2.9 MeV stabilizes with higher  $\lambda$  values. These effects indicate of the need of strong orthogonality conditions in the system. For further details, including the parameters set for the potential, we refer the reader to Refs. [4, 5].

## 3 Applications of MCAS theory

### 3.1 Analyzing powers of nucleons off ${}^{12}\text{C}$

Analyses of  $n-{}^{12}\text{C}$  system were published in Refs. [4, 5, 6]. Note that all the parameters, including the spin-orbit term, have been fixed on the known spectrum of  ${}^{13}\text{C}$ . Shortly after our analyses have been completed, new spin-polarization data measured at TUNL

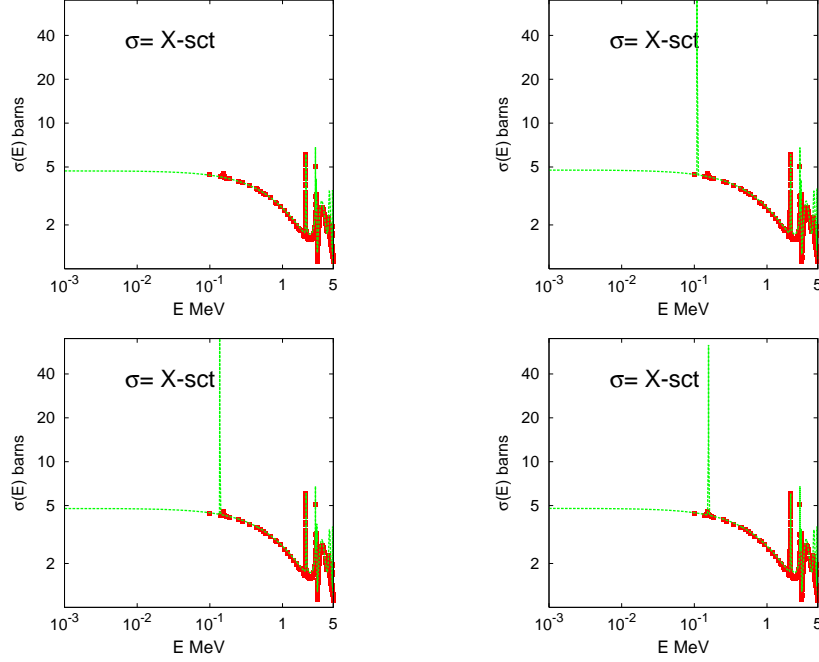


Figure 3: The  $\lambda$  dependence (of the elastic cross section for  $n$ - $^{12}\text{C}$  scattering) with values 100, 300, 500, and 1000 Mev (top-left, top-right, bottom-left and bottom-right, respectively)

$V_0^{(\pm)} = -45.0 \text{ MeV}$	$V_{ll}^{(\pm)} = 0.42 \text{ MeV}$	$V_{ls}^{(\pm)} = 7.0 \text{ MeV}$
$R_0 = 3.1 \text{ fm}$	$a_0 = 0.65 \text{ fm}$	$\beta_2 = -0.50$

Table 1: Coupled-channel parameters for  $n$ - $^{14}\text{C}$ /p- $^{14}\text{O}$

were published [12]. Without any parameter adjustments or tuning, we could reproduce those low-energy data, as shown in Fig. 4. Thus, this was a test of our spin-orbit parametrization and a validation of the spin-structure of our interaction [13].

### 3.2 Low-lying unbound states of $^{15}\text{C}$ and $^{15}\text{F}$

Our second analysis concerned an unbound nucleus,  $^{15}\text{F}$ , whose properties were studied in connection with its weakly-bound mirror partner  $^{15}\text{C}$ . Our analysis was triggered by recent low-energy experimental data on the  $^{14}\text{O}$ -proton system, which we could analyze by using inverse kinematics. We included in the model low-lying excitations of  $^{14}\text{O}/^{14}\text{C}$ , in a macroscopic coupled-channel model with parameters given in Table 1.

Our results are shown in Fig. 5. In the evaluations, we used known properties of  $^{15}\text{C}$  to predict new states in  $^{15}\text{F}$ , in particular three narrow resonances of negative parity ( $1/2^-$ ,  $5/2^-$  and  $3/2^-$  in the range 5-8 MeV). To obtain these results, a new concept had to be introduced [14]: it is the concept of Pauli-hindered states. Up to now we have considered states that are Pauli allowed ( $\lambda \simeq 0$ ) or Pauli forbidden ( $\lambda \geq 1\text{GeV}$ ). Now we introduce a state that is neither prohibited nor allowed but simply suppressed, or *hindered*, by the Pauli principle. We expect that this situation can apply in weakly-

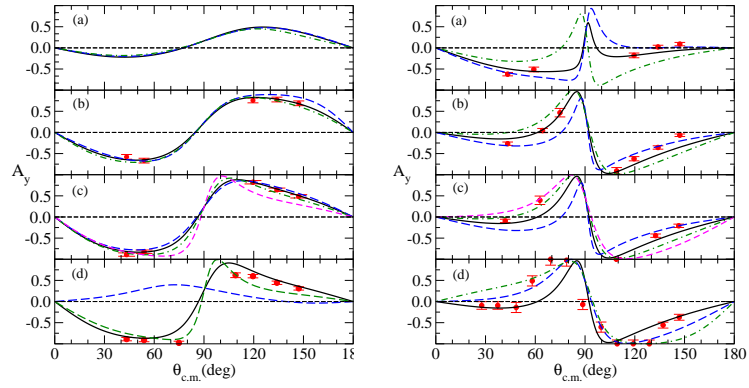


Figure 4: Neutron analyzing power  $A_y$  at various lab energies in the MeV ranges (a) 1.9, (b) 2.2, (c) 2.8, (d) 3.2 for the left panel, and (a) 3.41, (b) 3.62, (c) 3.78, (d) 3.92 for the right panel.

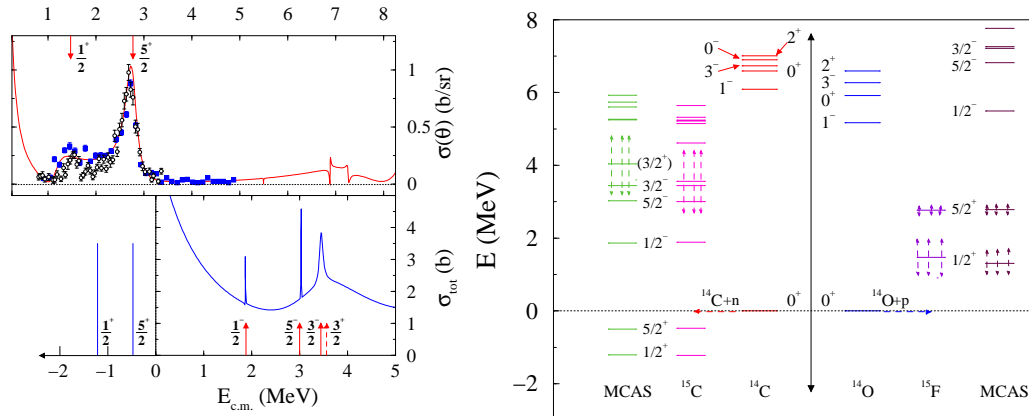


Figure 5: *Left:*  $^{15}\text{F}$  (top,  $p-^{14}\text{O}$  differential cross-section  $\theta_{cm} = 180^\circ$ ) &  $^{15}\text{C}$  (bottom, the bound spectrum and the elastic scattering cross-section). *Right:* The resonant spectra for  $^{15}\text{C}$  and  $^{15}\text{F}$

bound/unbound light systems where the formation of shells may become critical. These hindered states can be conveniently described in the OPP scheme with values of  $\lambda$  of a few MeV. Thus the scheme of phase-space that is accessible to the proton interacting with the  $^{14}\text{O}$  core is:

PAULI FORBIDDEN ( $\lambda \simeq 1\text{GeV}$ ):

$$\begin{array}{ccc} 0s_{1/2} + 0_1^+ & 0s_{1/2} + 0_2^+ & 0s_{1/2} + 2_1^+ \\ 0p_{3/2} + 0_1^+ & 0p_{3/2} + 0_2^+ & 1p_{3/2} + 2_1^+ \\ 0p_{1/2} + 0_1^+ & - & - \end{array}$$

PAULI HINDERED ( $\lambda \simeq 1 - 50\text{MeV}$ ):

$$\begin{array}{ccc} - & 0p_{1/2} + 0_2^+ & 0p_{1/2} + 2_1^+ \end{array}$$

PAULI ALLOWED ( $\lambda = 0\text{MeV}$ ):

$$\begin{array}{ccc} 1s_{1/2} + 0_1^+ & 1s_{1/2} + 0_2^+ & 1s_{1/2} + 2_1^+ \\ 0d_{5/2} + 0_1^+ & 0d_{5/2} + 0_2^+ & 0d_{5/2} + 2_1^+ \\ 0d_{3/2} + 0_1^+ & 0d_{3/2} + 0_2^+ & 0d_{3/2} + 2_1^+ \\ \dots & \dots & \dots \end{array}$$

The need to consider intermediate situations between Pauli blocking and Pauli allowance has been registered before in the literature, mostly in connection with RGM approaches [15, 16].

### 3.3 P-shells in mass=7 nuclei

As a third application, we consider the spectral structure the mass=7 isobars:  $^7\text{He}$ ,  $^7\text{Li}$ ,  $^7\text{Be}$ , and  $^7\text{B}$ . We describe these systems in terms of a single nucleon-nucleus interaction, explicitly including the low-lying core excitations of the mass-6 sub-system. Thus, we use the MCAS approach to determine the bound and resonant (above nucleon emission) spectra starting from a collective coupled-channel interaction model coupling the *g.s.* of  $^6\text{He}$  to the first and second  $2^+$  excitations. This description of the mass-7 systems is in many ways alternative to those based on cluster models ( $^7\text{Li}$  as a  $^3\text{H} + \alpha$  dicluster, etc.) or to those based on more microscopic models, either no-core shell-model or Green's function Montecarlo calculations. A comparison amongst different descriptions (dicluster model, no-core shell model, and collective-coupling model) for mass-7 nuclei is given in Ref. [17]. In the collective-coupling model, the four  $A=7$  nuclei are described in terms of the system *nucleon + mass-6-type nucleus* with a potential whose parameters are listed in Table 2:

$$\begin{array}{ll} ^7\text{Li} \leftrightarrow p & + \quad ^6\text{He}(0_1^+[g.s.]; 2_1^+[1.78\text{MeV}]; 2_2^+[5.6\text{MeV}]) \\ ^7\text{He} \leftrightarrow n & + \quad ^6\text{He}(0_1^+[g.s.]; 2_1^+[1.78\text{MeV}]; 2_2^+[5.6\text{MeV}]) \\ ^7\text{Be} \leftrightarrow n & + \quad ^6\text{Be}(0_1^+[g.s.]; 2_1^+[1.70\text{MeV}]; 2_2^+[5.6\text{MeV}]) \\ ^7\text{B} \leftrightarrow p & + \quad ^6\text{Be}(0_1^+[g.s.]; 2_1^+[1.70\text{MeV}]; 2_2^+[5.6\text{MeV}]) \end{array}$$

In Table 3 are shown the results obtained [17] with that CC nucleon-nucleus potential model. One CC potential model has been used for all four nuclides. The results



$V_0 = -36.817$	$V_{\ell\ell} = -1.2346$	$V_{\ell s} = 14.9618$	$V_{Is} = 0.8511$
$R_0 = 2.8 \text{ fm};$	$a = 0.88917 \text{ fm};$	$\beta_2 = 0.7298$	

Table 2: Parameter values of the nucleon-nucleus(mass-6) potential.

$J^\pi$	${}^7\text{Li}$		${}^7\text{Be}$	
	Exp.	Theory	Exp.	Theory
$0^+$	-9.975	-9.975	-10.676	-11.046
$1^-$	-9.497	-9.497	-10.246	-10.680
$2^-$	-5.323 [0.069]	-5.323	-6.106 [0.175]	-6.409
$3^-$	-3.371 [0.918]	-3.371	-3.946 [1.2]	-4.497
$4^-$	-2.251 [0.08]	-0.321	-3.466 [0.4]	-1.597
$5^-$	-1.225 [4.712]	-2.244	---	---
$6^-$	-0.885 [2.752]	-0.885	---	-2.116
$7^-$	-0.405 [0.437]	-0.405	-1.406 [?]	-1.704
$8^-$	---	---	-0.776 [1.8]	-3.346
$9^-$	1.265 (0.26)	0.704 (0.056)	0.334 (0.32)	-0.539
$10^-$	---	1.796 (1.57)	---	0.727 (0.699)
$11^-$	3.7 (0.8) ? <sup>a</sup>	2.981 (0.99)	---	1.995 (0.231)
$12^-$	4.7 (0.7) ? <sup>a</sup>	3.046 (0.75)	---	2.009 (0.203)
$13^-$	---	5.964 (0.23)	---	4.904 (0.150)
$14^-$	---	6.76 (2.24)	6.5 (6.5) ? <sup>a</sup>	5.78 (1.65)

$J^\pi$	${}^7\text{He}$		${}^7\text{B}$	
	Exp.	Theory	Exp.	Theory
$0^+$	0.445 (0.15)	0.43 (0.1)	2.21 (1.4)	2.10 (0.19)
$1^-$	---	1.70 (0.03)	---	3.01 (0.11)
$2^-$	1.0 (0.75) ? <sup>a</sup>	2.79 (4.1)	---	5.40 (7.2)
$3^-$	3.35 (1.99)	3.55 (0.2)	---	5.35 (0.34)
$4^-$	6.24 (4.0) ? <sup>a</sup>	6.24 (1.9)	---	---

Table 3: Experimental data and theoretical MCAS results for  ${}^7\text{Li}$  and  ${}^7\text{Be}$  states (left table), and for  ${}^7\text{He}$  and  ${}^7\text{B}$  (right table). All energies are in MeV and relate to scattering thresholds for nucleon+ ${}^6\text{He}$  or nucleon+ ${}^6\text{Be}$ . For states labeled by “?” spin-parity attributes are unknown or uncertain.

for  ${}^7\text{Li}/{}^7\text{Be}$  (and for  ${}^7\text{He}/{}^7\text{B}$ ) differ solely by the effect of the central Coulomb field. Instead, if we compare results for the pairs  ${}^7\text{Li}/{}^7\text{He}$  and  ${}^7\text{Be}/{}^7\text{B}$ , they differ solely for the different action of the OPP term. For the two mass-7 bound systems, Pauli blocking is assumed in the  $0s_{1/2}$  shells and all the remaining shells are considered allowed, while for the two unbound systems a more complex OPP scenario is considered: the  $0s_{1/2}$  shells are blocked, the  $p$  shells are hindered, and only the higher shells are completely allowed. This hindrance of the  $p$  shells could reflect the anomalous interaction of the neutron with  ${}^6\text{He}$ , which is a neutron halo. A similar situation could occur in the mirror case of  ${}^7\text{B}$ , with the interaction of a proton with a  ${}^6\text{Be}$ -type core. In our calculation, we have made the hypothesis of a Pauli hindrance in the p-shells defined by the following parameters:  $\lambda(0p_{3/2}[0_1^+; 2_1^+; 2_2^+]) = 17.6 \text{ MeV}$ ,  $\lambda(0p_{1/2}[0_1^+]) = 36.0 \text{ MeV}$ ,  $\lambda(0p_{1/2}[2_1^+; 2_2^+]) = 5.6 \text{ MeV}$ . The extended nature of the even-even mass-6 subsystems, either weakly-bound ( ${}^6\text{He}$ ) or unbound ( ${}^6\text{Be}$ ), is approximately reflected also in the geometric size of the potential parameters of Table 2, with rather extended radius, diffuseness, and quadrupole deformation.

## 4 Conclusions

The Sturmian-based MCAS approach has been applied to coupled-channel problems at low energy, using phenomenological potentials with macroscopic, collective-type, couplings. But the method is sufficiently flexible that it could be applied also in the presence of nonlocal potentials, such as those microscopically generated. Using simplified collective-type couplings, we have applied the approach to stable nuclei, as well as to weakly-bound and to unbound (with respect to the nucleon emission threshold) light nuclei. In the few cases considered, interesting results have been obtained, sometimes with rather good reproduction of bound spectra and scattering observables, and often

with predictions that could stimulate new experiments. In this approach, the highly nonlocal OPP term is crucial in order to include, macroscopically, the effects of Pauli exchanges. Finally, for weakly-bound or unbound light systems, the concept of Pauli hindrance is suggested. This implies that the nuclei have partially occupied  $p$ -shells or  $p$ -wave proto-shells wherein the Pauli principle neither forbids nor allows occupancy. To some extent, it represents a suppression of access to phase-space.

## References

- [1] S. Weinberg, Phys. Rev. **131**, 440 (1963); M. Scandron and S. Weinberg, Phys. Rev. **133** 1589 (1964).
- [2] J.T. Broad, Phys. Rev. A **31**, 1494 (1985); H. Marxer, S. Alston, and J. Briggs, J. Phys. D **8**, 177 (1988).
- [3] G.H. Rawitscher and L. Canton, Phys. Rev. C **44**, 60 (1991).
- [4] K. Amos, L. Canton, G. Pisent, J.P. Svenne, D. van der Knijff, Nucl. Phys. **A728**, 65 (2003).
- [5] L. Canton, G. Pisent, J.P. Svenne, D. van der Knijff, K. Amos, S. Karataglidis: Phys. Rev. Lett. **94**, 122503 (2005).
- [6] G. Pisent, J. P. Svenne, L. Canton, K. Amos, S. Karataglidis, and D. van der Knijff: Phys. Rev. C **72**, 014601 (2005).
- [7] C.V. Sukumar and D.M. Brink, J. Phys. A, **37** 5689 (2004).
- [8] S.Saito, Prog. Theor. Phys. **41** (1969) 705.
- [9] V.Kukulin and V.Pomerantsev, Annals of Phys. **111** (1978) 330.
- [10] E. Witten Nucl. Phys. B **188**, 513 (1981).
- [11] D. Baye, Phys. Rev. Lett. **58**, 2738 (1987).
- [12] C.D. Roper *et al.*, Phys. Rev. C **72**, 024605 (2005).
- [13] J. P. Svenne, K. Amos, S. Karataglidis, D. van der Knijff, L. Canton, and G. Pisent, Phys. Rev. C **73**, 027601 (2006).
- [14] L. Canton, G. Pisent, J.P. Svenne, K. Amos, S. Karataglidis: Phys. Rev. Lett. **96**, 072502 (2006).
- [15] E.W. Schmidt, in *Proceedings of the Workshop on Few-Body Problems in Nuclear Physics* Trieste, Italy, 1978. Edited by G. Pisent, V. Vanzani, L. Fonda (Trieste, IAEA, 1978), p. 389.
- [16] K. Langanke and H. Friedrich, Adv. Nucl. Phys. **17**, 223 (1986).
- [17] L. Canton, G. Pisent, K. Amos, S. Karataglidis, J.P. Svenne, and D. van der Knijff, arXiv:nucl-th/0604072 (2006), and Phys. Rev. C **74**, 064605 (2006).